The Astrophysical Journal, 668:L43–L46, 2007 October 10

THE ELONGATED STRUCTURE OF THE HERCULES DWARF SPHEROIDAL GALAXY FROM DEEP LARGE BINOCULAR TELESCOPE IMAGING[1]

Matthew G. Coleman,[2] Jelte T. A. de Jong,[2] Nicolas F. Martin,[2] Hans-Walter Rix,[2] David J. Sand,[3,4] Eric F. Bell,[2] Richard W. Pogge,[5] David J. Thompson,[6] H. Hippelein,[2] E. Giallongo,[7] R. Ragazzoni,[7] Andrea DiPaola,[7] Jacopo Farinato,[8] Riccardo Smareglia,[9] Vincenzo Testa,[7] Jill Bechtold,[3] John M. Hill,[6] Peter M. Garnavich,[10] and Richard F. Green[6]

Received 2007 June 11; accepted 2007 August 22; published 2007 September 24

ABSTRACT

We present a deep, wide-field photometric survey of the newly discovered Hercules dwarf spheroidal galaxy (dSph), based on data from the Large Binocular Telescope. Images in *B*, *V*, and *r* were obtained with the Large Binocular Camera covering a $23' \times 23'$ field of view to a magnitude of ~25.5 (5 σ). This permitted the construction of color-magnitude diagrams that reach approximately 1.5 mag below the Hercules main-sequence turnoff. Three-filter photometry allowed us to preferentially select probable Hercules member stars and to examine the structure of this system at a previously unattained level. We find that the Hercules dwarf is highly elongated (3 : 1), considerably more so than any other dSph satellite of the Milky Way, except the disrupting Sagittarius dwarf. Although we cannot rule out that the unusual structure is intrinsic to Hercules as an equilibrium system, our results suggest tidal disruption as a likely cause of this highly elliptical structure. Given the relatively large galactocentric distance of this system (132 ± 12 kpc), signs of tidal disruption would require the Hercules dwarf to be on a highly eccentric orbit around the Milky Way.

Subject headings: galaxies: individual (Hercules dwarf spheroidal galaxy) — galaxies: kinematics and dynamics

1. INTRODUCTION

At the lowest luminosity end of the realm of galaxies, dwarf spheroidal galaxies (dSph's) are characterized as low surface brightness systems that are highly dominated by dark matter and that have star formation histories ranging from the simple to the complex. The Milky Way (MW) currently has 18 known dSph companions; many of these, including the Hercules dwarf spheroidal galaxy (Belokurov et al. 2007), were recently discovered by the Sloan Digital Sky Survey (SDSS; Adelman-McCarthy et al. 2007). Each of these must be experiencing some structural distortion due to the MWs gravitational field, and tidal distortions and disruptions have been recognized in some of them, foremost the Sagittarius dSph (Ibata et al. 1994) but also the Ursa Minor (Martínez-Delgado et al. 2001; Palma et al. 2003) dSph. The nearby Coma Berenices and Ursa Major II dSph's also show tentative signs of distortion, which may be tidal in origin (Belokurov et al. 2007; Zucker et al. 2006; Grillmair 2006). However, the satellites >100 kpc from the Galactic center experience weaker tidal forces, and the level to which they are also tidally distorted is not clear; yet it is the pericentric distance of a satellite, not its current distance, that determines how much a satellite is affected by tides.

In this Letter, we present and analyze deep images of the recently discovered Hercules dSph, which lies at a distance of ~140 kpc (Belokurov et al. 2007). Belokurov et al. inferred that the Hercules dSph displays an extended morphology and may contain multiple stellar populations. A spectroscopic survey by Simon & Geha (2007) measured a mass-to-light ratio of 332 ± 221 in solar units and found evidence of kinematic substructure. In this Letter, we examine the structure of the Hercules dSph using photometry obtained with the newly commissioned Large Binocular Telescope. We demonstrate that the structure of Hercules is highly elongated, much more so than all other known distant dSph's, possibly indicating strong tidal distortion.

2. DEEP PHOTOMETRY FROM THE LBT

The Large Binocular Telescope is located on Mount Graham in Arizona, and it consists of two 8.4 m mirrors on a common mount (Hill et al. 2006). Our data were obtained as part of the LBT Science Demonstration Time, during which a single mirror of the LBT was fitted with the blue channel of the Large Binocular Camera (LBC; Ragazzoni et al. 2006; E. Giallongo et al. 2007, in preparation). The LBC is a wide-field imager that provides a $23' \times 23'$ field of view, sampled at 0.23 arcsec pixel^{-1} over four chips of 2048×4608 pixels. LBC-Blue is optimized for the UV–blue wavelengths, from 320 to 500 nm, and is equipped with the *U*, *B*, *V*, *g*, and *r* filters.

The Hercules dSph was imaged with the LBT/LBC-Blue setup on 2007 March 17 and May 13. The data consist of five 5 minute exposures in the Gunn *r* band, four 5 minute exposures in the *V*

[1] Based on data acquired using the Large Binocular Telescope (LBT). The LBT is an international collaboration among institutions in the US, Italy, and Germany. LBT Corporation partners are the University of Arizona, on behalf of the Arizona university system; Istituto Nazionale di Astrofisica, Italy; LBT Beteiligungsgesellschaft, Germany, representing the Max Planck Society, the Astrophysical Institute Potsdam, and Heidelberg University; Ohio State University; and the Research Corporation, on behalf of the University of Notre Dame, the University of Minnesota, and the University of Virginia.

[2] Max-Planck-Institut für Astronomie, Königstuhl 17, D-69117 Heidelberg, Germany.

[3] Steward Observatory, University of Arizona, Tucson, AZ 85721.

[4] *Chandra* Fellow.

[5] Department of Astronomy, Ohio State University, 140 West 18th Avenue, Columbus, OH 43210-1173.

[6] Large Binocular Telescope Observatory, University of Arizona, 933 North Cherry Avenue, Tucson, AZ 85721-0065.

[7] INAF, Osservatorio Astronomico di Roma, via Frascati 33, I-00040 Monteporzio, Italy.

[8] INAF, Osservatorio Astronomico di Padova, vicolo dell'Osservatorio, 5, 35122 Padova, Italy.

[9] INAF, Osservatorio Astronomico di Trieste, via G. B. Tiepolo, 11, 34131 Trieste, Italy.

[10] Harvard-Smithsonian Center for Astrophysics, 60 Garden Street, Cambridge MA 02138.

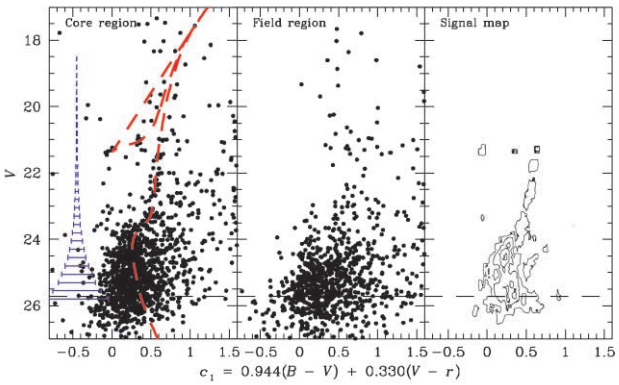

FIG. 1.—Color-magnitude diagrams for the central region of Hercules (*left panel*) and a field region of equivalent area on the sky (*middle panel*). The photometry has been corrected for extinction, and all sources outside the sharpness limit have been removed. Our principal color, c_1, has been designed to enhance the Hercules-to-field contrast in the color-magnitude plane. The red dashed line is the isochrone of a metal-poor stellar population at 13 Gyr (Girardi et al. 2002, 2004). The blue error bars in the left panel represent the uncertainty in the colur c_1 returned by the artificial-star tests, and the dashed lines trace the V magnitude at which the photometric completeness has fallen to 50%. The "signal-to-noise" ratio map of Hercules is shown in the right panel, where the contours represent signal values of 1.5, 3.0, 4.5, and 6.0. The limiting signal of $s = 3.0$ provided the CMD-selection region for the Hercules main-sequence population. Note the increased background galaxy contamination in the middle panel at magnitudes fainter than $V = 24$.

band, and six 5 minute exposures in the B band (all dithered), taken during photometric conditions with a seeing of approximately 0.8″–1.1″. The data were reduced using standard IRAF routines in the `mscred` package; the images on the four chips were trimmed and bias-subtracted, and they were then flat-fielded using the combined twilight flats obtained at the start of the night. The images contained significant field distortion at the edge, resulting from the "fast" focal ratio (f/1.14) of the LBTs primary mirrors. This was removed before co-adding the science frames, by applying a quadratic radial correction (accuracy 0.2″). The Hercules images were then median-combined using the `mscstack` and `mscskysub` routines (Valdes 2002) to produce the final science frames.

Photometry was measured using the PSF-fitting algorithm within the DAOPHOT package, from which we obtained 50,810 stars with B, V, and r photometry. The photometric data set was calibrated using stars from SDSS, bypassing any need for an atmospheric extinction correction. The zero-point uncertainties were $\delta r \sim 0.02$ mag and δB, $\delta V \sim 0.03$ mag, including the empirical color transformations described by Jordi et al. (2006), without any indication of zero-point gradients across the LBC field. We then corrected the photometry for extinction using the dust maps of Schlegel et al. (1998), with $\langle E(B - V)\rangle$ of 0.055 mag. The photometric uncertainty and completeness as functions of magnitude were assessed using artificial star tests. We placed 1600 artificial stars in the image and attempted to recover them with DAOPHOT, where the photometric uncertainty was then determined as the dispersion of the returned magnitudes about the mean (i.e., not the input). This was repeated for artificial stars at every 0.25 mag in the B, V, and r frames.

The resulting color-magnitude diagrams (CMDs) for selected regions of the image are shown in Figure 1. For our analysis of the Hercules dSph, we adopted the specially fit "colors," c_1 and c_2, which represent a combination of our three filter photometry in B, V, and r. These principal colors are designed to enhance the Hercules-to-field contrast in the CMD (see § 3), and they are similar to those used by Odenkirchen et al. (2001). By fitting a ridgeline locus in this plane, using the stars at the center of Hercules, we found the principal colors to be $c_1 = 0.944(B - V) + 0.330(V - r)$ and $c_2 = -0.330(B - V) + 0.944(V - r)$. A diagram in the ($c_2$, V)-plane is essentially the CMD seen edge-on, and the dispersion of Hercules member stars around $c_2 = 0$ is defined by the photometric errors. For the remainder of this Letter, our CMDs will be defined in the (c_1, V)-plane. The blue error bars in Figure 1 represent the combined uncertainty of the color c_1, and the dashed lines represent the magnitude at which the photometric completeness has fallen to 50%: $B_{50} = 25.60 \pm 0.05$ mag, $V_{50} = 25.72 \pm 0.05$ mag, and $r_{50} = 25.56 \pm 0.04$ mag.

TABLE 1
PROPERTIES OF THE HERCULES dSph

Parameter	Value
R.A. (J2000)	$16^h31^m02.0^s$
Decl. (J2000)	12°47′29.6″
$E(B - V)$	0.055 ± 0.005 mag[a]
$(m - M)_0$	20.6 ± 0.2 mag
Distance	132 ± 12 kpc
King r_h	$4.37' \pm 0.29'$ (168 ± 19 pc)
King r_c	$4.74' \pm 0.57'$ (182 ± 27 pc)
King r_t	$25.9' \pm 11.1'$ [$(1.0 \pm 0.4) \times 10^3$ pc]
$c = \log(r_t/r_c)$	0.74 ± 0.25

[a] The uncertainty quoted here represents the variation in reddening over the LBT field (Schlegel et al. 1998).

3. THE STRUCTURE OF HERCULES

The CMD of all stellar sources in the Hercules core region is shown in Figure 1, the first data for this galaxy to reach well below the main-sequence turnoff. Based on the B and V photometry, and using the CMD-fitting techniques developed by Dolphin (2002), we constrained the star formation history of Hercules. The results imply the presence of only a single, ancient (>10 Gyr) population of stars with no significant subsequent star formation episodes. We derived the best-fitting distance, age, and metallicity for such a single stellar population (Table 1) using the methods described by de Jong et al. (2007). The dashed line in Figure 1 traces the isochrone for a stellar population with an [Fe/H] abundance of −2.26 and an age of 13 Gyr (Girardi et al. 2002, 2004).

Starting from the CMD of all detected sources in the entire field, we tried to isolate probable Hercules dSph stars by excising "field sources," such as foreground stars and background galaxies, using a CMD-selection technique originally introduced by Grillmair et al. (1995; see also Odenkirchen et al. 2001): a comparison was made between the (c_1, V) CMD of the central region of Hercules and that of the field region (a distant portion of the 23′ × 23′ field of view) to produce a "signal-to-noise" ratio map of the Hercules stellar population across the CMD (the right panel of Fig. 1). The CMDs for the core of Hercules and the field are shown in Figure 1, where the associated spatial regions were chosen iteratively and are outlined in Figure 2. To make a map of probable Hercules member stars (Fig. 2), we then chose a limiting signal-to-noise ratio in the CMD plane ($s = 3.0$, the second contour in the right panel of Fig. 1) that minimized the field population while maintaining a high number of Hercules stars. This corresponds to the main-sequence turnoff and upper main-sequence region of the Hercules CMD; only stars above the 50% completeness limit shown in Figure 1 were selected.

At such faint magnitudes, background galaxies form the ma-

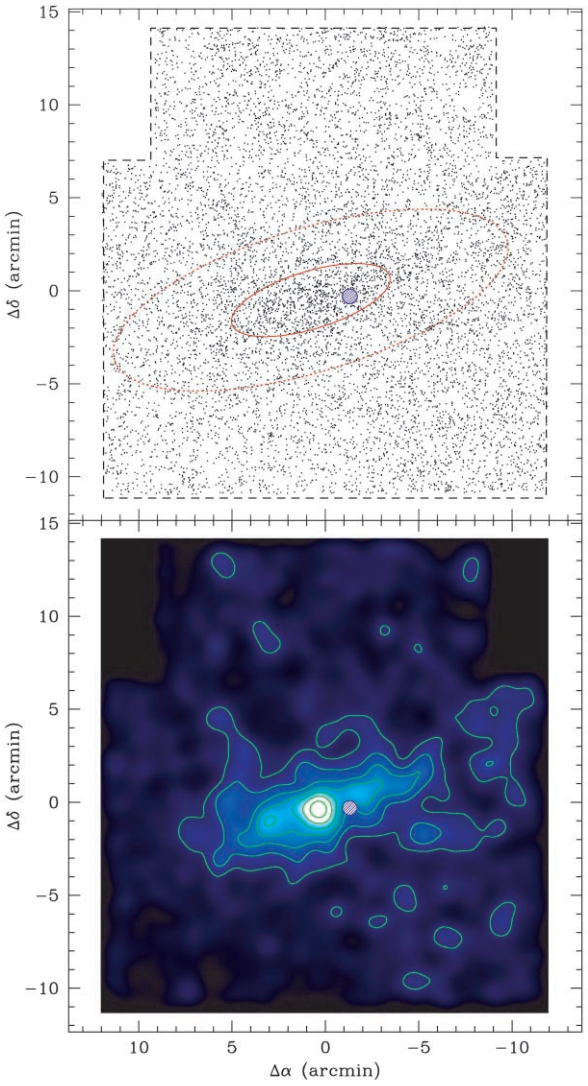

FIG. 2.—*Upper panel:* Spatial distribution of the Hercules CMD-selected objects, where the dashed line marks the limit of our LBT data. The blue shaded region represents the saturated star aligned toward the center of the dSph. The solid red ellipse marks the core radius from our best-fitting King model (see Fig. 3), and the dashed ellipse outlines the inner border of the field region. Both the core and field populations were used to derive the CMD-selection limit shown in Fig. 1. These ellipses have an ellipticity of 0.65 and semi-major axis radii of 4.42′ and 11′, respectively. *Lower panel:* Contour diagram of the CMD-selected sources. Each star has been convolved with a Gaussian of width 0.6′. The contours correspond to stellar densities of 1.5 σ, 3 σ, …, 10.5 σ above the background, where σ is the uncertainty in the background stellar density from Poisson statistics.

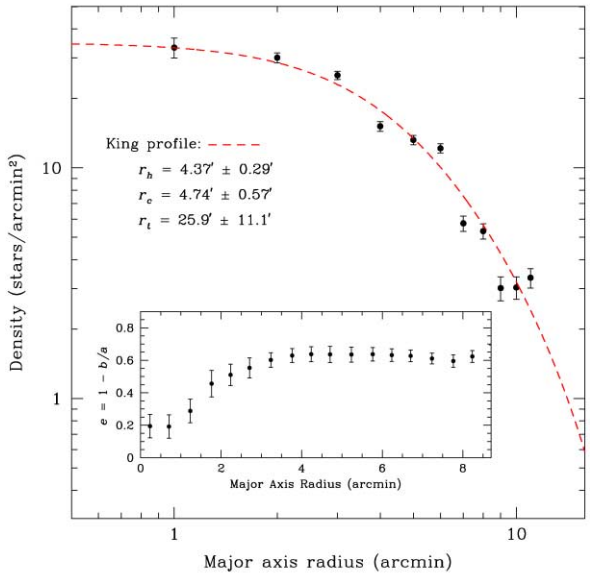

FIG. 3.—Radial profile of Hercules, determined from the CMD-selected data set. The stellar density was evaluated within ellipses at every 1′ major axis radius using an ellipticity of 0.65 and a position angle of −73°. The dashed line represents the best-fitting King profile, and the parameters with their associated bootstrap uncertainties are listed. The background level of 15.43 ± 0.28 stars arcmin^{-2} (Poisson statistical uncertainty) has been subtracted from all data points. *Inset*: Ellipticity as a function of radius. Uncertainties were determined using bootstrap resampling. The central coordinates of this system demonstrate a mild dependence on radius, with a variation of ∼0.3′ in R.A. and ∼0.2′ in decl. over the radial range.

jority of contaminating sources, and, consequently, optimal star-galaxy separation is important. The FWHM of many background galaxies are expected to be significantly larger than that of a star; hence, the DAOPHOT "sharpness" parameter provided a secondary level of filtering. We used the sharpness values from the *B*-band image, for which the point-spread function (PSF) shape was effectively constant across the field and for which the seeing was best (0.8″). We constructed a sharpness map across the LBT *B*-band image using the bright stars ($14 \leq B \leq 22$) and removed all sources with a nonstellar sharpness. These nonstellar objects were evenly distributed across the imaged area, which suggests that they are field objects. Together, the CMD-selection and star-galaxy separation techniques removed 85% of the field population stars. Our final Hercules data consisted of 10,033 stars.

The spatial distribution of the "cleaned" Hercules data set is shown in Figure 2 (*upper panel*). A relatively bright star ($g = 15.5$; SDSS) near the center of the Hercules dSph is saturated in our data. The data in this region were excluded from our analysis. We converted this map into a stellar surface density contour diagram (Fig. 2, *lower panel*) by convolving each star with a Gaussian of radius 0.6′ (independent of stellar magnitude), where the contours trace stellar densities of 1.5 σ, 3 σ, …, 10.5 σ above the field density (σ is the variance of the mean background level within a circle of radius 0.6′).

Both panels in Figure 2 show a strikingly elongated stellar distribution of the Hercules dSph. We quantified the internal structure of Hercules by fitting a series of radially increasing elliptical contours to the stellar density map displayed in Figure 2, using the IRAF routine `ellipse`. The best-fitting position angle, ellipticity, and central coordinates were measured at semimajor radii of 0.25′, 0.75′, …, 9.75′ for 200 random data subsets (50% of all stars), with associated uncertainties calculated using bootstrap sampling. The results in Figure 3 indicate that the ellipticity of Hercules is relatively mild toward the center[11] ($e \sim 0.3$); however, this increases sharply to an ellipticity of $e \sim 0.65$ in the outer regions. That is, the major–to–minor-axis ratio of Hercules is approximately 3 : 1, flatter than any other known Milky Way dSph, except the tidally disrupted nearby Sagittarius dSph.

We also constructed an azimuthally averaged stellar density

[11] Our measurement for the ellipticity of the inner regions is likely to be a lower limit due to the "blurring" effect of the Gaussian convolution function described above. Also, the ellipticity is measured in the plane of the sky, and Hercules may be further elongated along the line of sight.

radial profile of the dSph in a series of concentric annuli (separated by 0.5′, with a fixed ellipticity of $e = 0.65$ and position angle of −73°). The background level was calculated as the density of stars in the upper ($\Delta\delta \geq 8'$) and lower ($\Delta\delta \leq -5'$) regions of the LBT field. This was subtracted from the profile data points, and the result is shown in Figure 3. We derived a best-fitting King (1962) profile for this system using bootstrap resampling, yielding a half-light (major-axis) radius of $4.37' \pm 0.29'$ (168 ± 19 pc), a core radius of $4.74' \pm 0.57'$ (182 ± 27 pc), and a tidal radius of $25.9' \pm 11.1'$ [$(1.0 \pm 0.5) \times 10^3$ pc]. Note that the formal tidal radius of the Hercules dSph is beyond the spatial range of our data set and should be treated with caution.

4. DISCUSSION

In their discovery paper, Belokurov et al. (2007) examined the Hercules structure based on photometry complete to $i \sim 22.5$ (the depth of the subgiant branch) and found that the system has an extended elongated morphology with an ellipticity of $e \sim 0.5$ (a major–to–minor-axis ratio of 2 : 1). In our analysis, we have probed ∼3 mag deeper, allowing for a structural map of much greater signal-to-noise ratio. Our data clearly confirm that this object is highly elongated (3 : 1) and shows some tentative indication of clumpy substructure[12] (see Fig. 2).

We can reproduce the analysis of Belokurov et al. (2007) by repeating the CMD selection for a data set with a brightness limit of $V = 23$, which comprises only the Hercules red giant branch. This bright-limit data set contains <100 Hercules member stars, as compared to ∼1500 members for the faint-limit data set described in the previous section. When using the bright limit, we find an *average* ellipticity of $e = 0.52$, consistent with the Belokurov et al. measurement. However, the uncertainty associated with this value is considerable (∼0.2) due to the small number of dSph stars: the ellipticity ranges from 0.31 to 0.75 in the core, and the signal of Hercules becomes too low for an accurate measurement beyond $r = 4'$. We also note that the ellipticity measurement in the central region is a lower limit, due to the "blurring" effect of the Gaussian convolution function. Similarly, for our deep data set, we do not believe the inner three ellipticity data points in Figure 3 reflect the true structure of the Hercules core. These tests demonstrate that our data are fully consistent with the results of Belokurov et al.; however, the large number of member stars from the deep observations presented here is necessary to robustly measure the high degree of flattening

[12] Note that the visual impression of substructure in Fig. 2 is affected by the presence of the bright star, which is represented by the blue shaded region.

It is possible that the elongated structure of Hercules is intrinsic to this system. If so, it would be the most flattened of all the Milky Way dSph's (except the Sagittarius dSph). All other known stellar systems with 3 : 1 flattening or more are predominately supported by rotation, yet no stellar system with a characteristic velocity as low as Hercules ($\sigma \sim 5$ km s^{-1}; Simon & Geha 2007) is known to be rapidly rotating. If in equilibrium, Hercules would have unique structural or kinematic properties.

Structurally, the Hercules dSph most closely resembles the Ursa Minor dSph ($e \sim 0.56$), a Milky Way satellite that is presumably disrupting (Martínez-Delgado et al. 2001; Palma et al. 2003). The only other highly elliptical Milky Way dSph is the Sagittarius system, a relatively bright dSph that is being disrupted by Galactic tidal forces. Tidal forces could therefore be a plausible explanation for the elongated Hercules structure. However, the large distance of Hercules is problematic for this interpretation. Tidal forces decrease as R^{-3}, and the presence of tidal distortion would imply that Hercules is on a highly elliptical orbit around the Milky Way, to allow the system to experience strong tidal forces during its pericentric passage.

A simple condition for tidal disruption of Hercules at its orbital pericenter, $R_{\rm peri}$, is $\sigma_{\rm Herc}/r_{\rm Herc} \approx \sigma_{\rm MW}/R_{\rm peri}$, where $\sigma_{\rm Herc}$ and $\sigma_{\rm MW}$ are the velocity dispersions of the Hercules dSph and the Milky Way, respectively, and $r_{\rm Herc}$ is the limiting radius of Hercules. For $r_{\rm Herc} \sim 250$ pc (i.e., the geometric mean of the major and minor axes), $\sigma_{\rm Herc} \sim 5.1$ km s^{-1} (Simon & Geha 2007), and $\sigma_{\rm MW} \sim 150$ km s^{-1}, we find that only $R_{\rm peri} \sim 8$ kpc would lead to disruption. Given that Hercules is now located at a distance of 132 kpc (and may not yet be at apogalacticon), this would imply an orbit for this system of extreme ellipticity, $e > 0.9$. A simple method for estimating the *minimum* orbital eccentricity is provided by Oh et al. (1995), who assumed that the galactocentric radial velocity of the system is at its maximum. From the Simon & Geha (2007) value (144.6 km s^{-1}), we find $e_{\rm min} \gtrsim 0.5$. A detailed analysis of the feasibility and plausibility of this scenario is warranted but is beyond the scope of this Letter. At any rate, regardless of whether Hercules's highly flattened structure is due to tides, which appears on balance most plausible, or intrinsic to an equilibrium system, its properties are exceptional.

The authors thank the LBT Science Demonstration Time (SDT) team for assembling and executing the SDT program. We also thank the LBC team and the LBTO staff for their kind assistance. M. G. C. acknowledges the assistance of Roland Gredel in accessing LBT data, and that of Tom Herbst in the preparation of this Letter. The authors thank Dennis Zaritsky and Matthias Steinmetz for their helpful comments on the manuscript.

REFERENCES

Adelman-McCarthy, J. K., et al. 2007, ApJS, in press
Belokurov, V., et al. 2007, ApJ, 654, 897
de Jong, J. T. A., Rix, H., Martin, N. F., Zucker, D. B., Dolphin, A. E., Bell, E. F., Belokurov, V., & Evans, N. W. 2007, AJ, submitted (astro-ph/0708.3758)
Dolphin, A. E. 2002, MNRAS, 332, 91
Girardi, L., Bertelli, G., Bressan, A., Chiosi, C., Groenewegen, M. A. T., Marigo, P., Salasnich, B., & Weiss, A. 2002, A&A, 391, 195
Girardi, L., Grebel, E. K., Odenkirchen, M., & Chiosi, C. 2004, A&A, 422, 205
Grillmair, C. J. 2006, ApJ, 645, L37
Grillmair, C. J., Freeman, K. C., Irwin, M., & Quinn, P. J. 1995, AJ, 109, 2553
Hill, J. M., Green, R. F., & Slagle, J. H. 2006, Proc. SPIE, 6267, 62670Y
Ibata, R. A., Gilmore, G., & Irwin, M. J. 1994, Nature, 370, 194
Jordi, K., Grebel, E. K., & Ammon, K. 2006, A&A, 460, 339
King, I. 1962, AJ, 67, 471
Martínez-Delgado, D., Alonso-García, J., Aparicio, A., & Gómez-Flechoso, M. A. 2001, ApJ, 549, L63
Odenkirchen, M., et al. 2001, AJ, 122, 2538
Oh, K. S., Lin, D. N. C., & Aarseth, S. J. 1995, ApJ, 442, 142
Palma, C., Majewski, S. R., Siegel, M. H., Patterson, R. J., Ostheimer, J. C., & Link, R. 2003, AJ, 125, 1352
Ragazzoni, R., et al. 2006, Proc. SPIE, 6267, 626710
Schlegel, D. J., Finkbeiner, D. P., & Davis, M. 1998, ApJ, 500, 525
Simon, S. D., & Geha, M. 2007, ApJ, submitted (astro-ph/0706.0516)
Valdes, F. G. 2002, in Automated Data Analysis in Astronomy, ed. R. Gupta, H. P. Singh, & C. A. L. Bailer-Jones (New Delhi: Narosa Publ. House), 309
Zucker, D. B., et al. 2006, ApJ, 650, L41